Open
ORIGINAL ARTICLE

Cell Research (2016) 26:645-654.
www.nature.com/cr

Vertical transmission of Zika virus targeting the radial glial cells affects cortex development of offspring mice

Kong-Yan Wu[1, *], Guo-Long Zuo[1, 3, *], Xiao-Feng Li[2, *], Qing Ye[2], Yong-Qiang Deng[2], Xing-Yao Huang[2], Wu-Chun Cao[2], Cheng-Feng Qin[2], Zhen-Ge Luo[1, 3, 4]

[1]Institute of Neuroscience, State Key Laboratory of Neuroscience, Shanghai Institutes for Biological Sciences, Center for Excellence in Brain Science and Intelligence Technology, Chinese Academy of Sciences, Shanghai 200031, China; [2]Department of Virology, State Key Laboratory of Pathogen and Biosecurity, Beijing Institute of Microbiology and Epidemiology, Beijing 100071, China; [3]Chinese Academy of Sciences University, Beijing, China; [4]ShanghaiTech University, Shanghai, China

The recent Zika virus (ZIKV) epidemic in Latin America coincided with a marked increase in microcephaly in newborns. However, the causal link between maternal ZIKV infection and malformation of the fetal brain has not been firmly established. Here we show a vertical transmission of ZIKV in mice and a marked effect on fetal brain development. We found that intraperitoneal (i.p.) injection of a contemporary ZIKV strain in pregnant mice led to the infection of radial glia cells (RGs) of dorsal ventricular zone of the fetuses, the primary neural progenitors responsible for cortex development, and caused a marked reduction of these cortex founder cells in the fetuses. Interestingly, the infected fetal mice exhibited a reduced cavity of lateral ventricles and a discernable decrease in surface areas of the cortex. This study thus supports the conclusion that vertically transmitted ZIKV affects fetal brain development and provides a valuable animal model for the evaluation of potential therapeutic or preventative strategies.

***Keywords*:** Zika virus; vertical transmission; radial glial cells; cortical development
Cell Research (2016) **26**:645-654. doi:10.1038/cr.2016.58; published online 13 May 2016

Introduction

Zika virus (ZIKV), a positive single-strand RNA flavivirus spread by infected mosquitoes, is usually considered to cause asymptomatic infections or only mild symptoms, including fever, malaise, rash and conjunctivits, and in rare cases Guillain-Barre syndrome mediated by immune reactions damaging the peripheral nervous system [1-3]. The recent outbreak of ZIKV infection in the Americas, in particular Brazil, is accompanied by a marked increase in cases of microcephaly of newborns [4-7], and several case reports have shown the presence of ZIKV particles in the microcephalic fetal brain [8-10]. On the basis of the potential threat of ZIKV infection on central nervous system development of infants, the World Health Organization declared in February 2016, the danger of ZIKV on pregnancy as a Public Health Emergency of International Concern (PHEIC) [11].

Although epidemiologic retrospective studies indicate correlation between reports of suspected microcephaly with ZIKV incidence [12, 13], causal link has been debated because complex chemical or other environmental factors may also cause similar defects. Recently, three independent studies have determined the effects of ZIKV on cultured human neural progenitors or 3D organoids, which were derived from induced pluripotent stem (iPS) cells, and found that ZIKV specifically infected these *in vitro* cultured neural progenitors and inhibited their proliferation [14-16]. Another report using single-cell gene expression analysis suggested the expression of a candidate ZIKV receptor in diverse cell types, including radial glial (RG) cells, in developing nervous system of various species [17]. Although these lines of evidence are consistent with observed microcephaly in infected fetuses, there is an urgent need for the development of an animal model to firmly establish the link between vertical ZIKV infection and malformation of the fetal brain.

*These three authors contributed equally to this work.
Correspondence: Zhen-Ge Luo[a], Cheng-Feng Qin[b]
[a]E-mail: zgluo@ion.ac.cn
[b]E-mail: qincf@bmi.ac.cn
Received 24 April 2016; revised 30 April 2016; accepted 2 May 2016; published online 13 May 2016

Here we show that maternally infected ZIKV can cross the mouse placental barrier, infect radial glial cells of the fetal brain, and cause either directly or indirectly a reduction in the proliferative pool of cortical neural progenitors, leading to a discernable brain developmental defect in offspring mice. This work establishes the causal link between maternal ZIKV infection and malformation of the fetal brain in a mouse model.

Results

Vertically transmitted ZIKV targets radial glial cells of fetal mice

ZIKV can be classified into African and Asian genotypes [18]. The widespread ZIKV epidemic from 2015 to present in Latin America is caused by the Asian type strains [12]. In this study, we used a contemporary Asian ZIKV strain SZ01 (GenBank accession no: KU866423) isolated from the acute phase serum of a Chinese male patient returning from Samoa in 2016 [19], where ZIKV transmission was reported in 2015 [20]. To determine whether ZIKV infects mouse neural progenitors, we injected the virus into the lateral ventricle of fetal mice at embryonic day 13.5 (E13.5) and analyzed the distribution of viruses on E17.5 and postnatal day 1 (P1) (Figure 1A). Interestingly, we found that the cells in the ventricular zone (VZ) of dorsal telencephalon exhibited strong virus signals, detected by immunostaining with the patient's convalescent phase serum (Figure 1B, middle row, left two images). We also observed virus signals in the striatum (Figure 1B, middle row, right two images).

Because ZIKV is suspected to be able to cross the human fetal-placental barrier and infect the developing fetal brain [8, 21, 22], we aimed to set up a vertical transmission model of ZIKV infection in immunocompetent mice. We injected ZIKV intraperitoneally (i.p.) into pregnant mice at E13.5 and determined the distribution of viruses in the offspring mice (Figure 1A). We found that upon i.p. inoculation, ZIKV could efficiently establish a transient viremia on day 1 post infection in pregnant mice (Figure 1C). In particular, ZIKV-specific RNA was detected in 5 out of 9 placentas on day 3 post infection (Figure 1D). Surprisingly, we found that the ZIKV signals were specifically distributed in the dorsal VZ of the fetal brain (Figure 1B, bottom row, left two images), but not in other brain regions including striatum (Figure 1B, bottom row, right two images). These results suggest that ZIKV can efficiently cross the mouse fetal-placental barrier and that the cortical neural progenitors of fetal mice are the specific target of vertically transmitted ZIKV. In line with this conclusion, most ZIKV signals were co-localized with BLBP, a marker of radial glia (RG) cells, the major cortical neural progenitors localized in the VZ (Figure 1E and 1F). Thus, RG cells are the primary targets of ZIKV in infected fetal mouse brains. In line with this conclusion, ZIKV signals were usually distributed as granular patterns in cytoplasmic regions of cells postively labeled by Pax6, another marker of RG cells (Supplementary information, Figure S1), or Sox2, a transcription factor essential for maintaining cell stemness potency (Figure 1E).

ZIKV infection abolishes proliferative pool of cortical neural progenitors in fetal mice

We next determined effects of ZIKV infection on cortical neural progenitors of the fetal brain. We first stained fetal brain slices with Ki67, a marker for mitotic cells, and found that ZIKV infection markedly reduced the number of Ki67-positive cells in VZ/subventricular zone (SVZ) and intermediate zone (IZ) (Figure 2A and 2B). This result suggests an inhibitory effect of ZIKV on proliferation of cortical neural progenitors. We also observed a marked decrease in the intensity and band thickness of cells positively-labeled by BLBP or Sox2 (Figure 2C-2E), suggesting the reduction of cortical neural progenitor pool upon ZIKV infection. These results are in agreement with the findings that ZIKV induces cell death and inhibits cell cycle progression in cultured human cortical neural progenitors [14].

In the mouse SVZ, the intermediate progenitors (IPs)

Figure 1 Vertical transmission of ZIKV and targeting of radial glia cells in fetal mice. **(A)** Experimental procedures of ZIKV infection in mouse. ZIKV was intraperitoneally (i.p.) injected into pregnant C57 mice at E13.5 or directly injected into the lateral ventricle of the fetus, followed by brain examination on E17.5 or P1. **(B)** P1 mouse brain slices were stained with convalescent phase serum and DAPI which labels the nucleus. Shown are representative images from 5 mice. Note the virus signals in VZ regions in ZIKV-injected group and nonspecific background signal in mock i.p. injected group. Scale bar, 100 μm. **(C)** Viremia of ZIKV-infected mice by i.p. route. Pregnant mice were inoculated with ZIKV, and viremia was determined on 1, 2 and 3 days post inoculation by real-time RT-PCR. Dotted lines represent limits of detection. **(D)** Placenta of each embryo was collected at 3 days post inoculation and viral titers was determined by real-time RT-PCR. Dotted line represents limits of detection. **(E)** Immunostaining for radial glia marker BLBP and stem cell marker Sox2 in brain slices from P1 mice i.p injected with ZIKV at E13.5. Arrows indicate ZIKV and BLBP colocalized signals. Scale bar, 50 μm. **(F)** Quantification of the percentage of ZIKV signals colocalized with BLBP. Data are the average of five mouse brains.

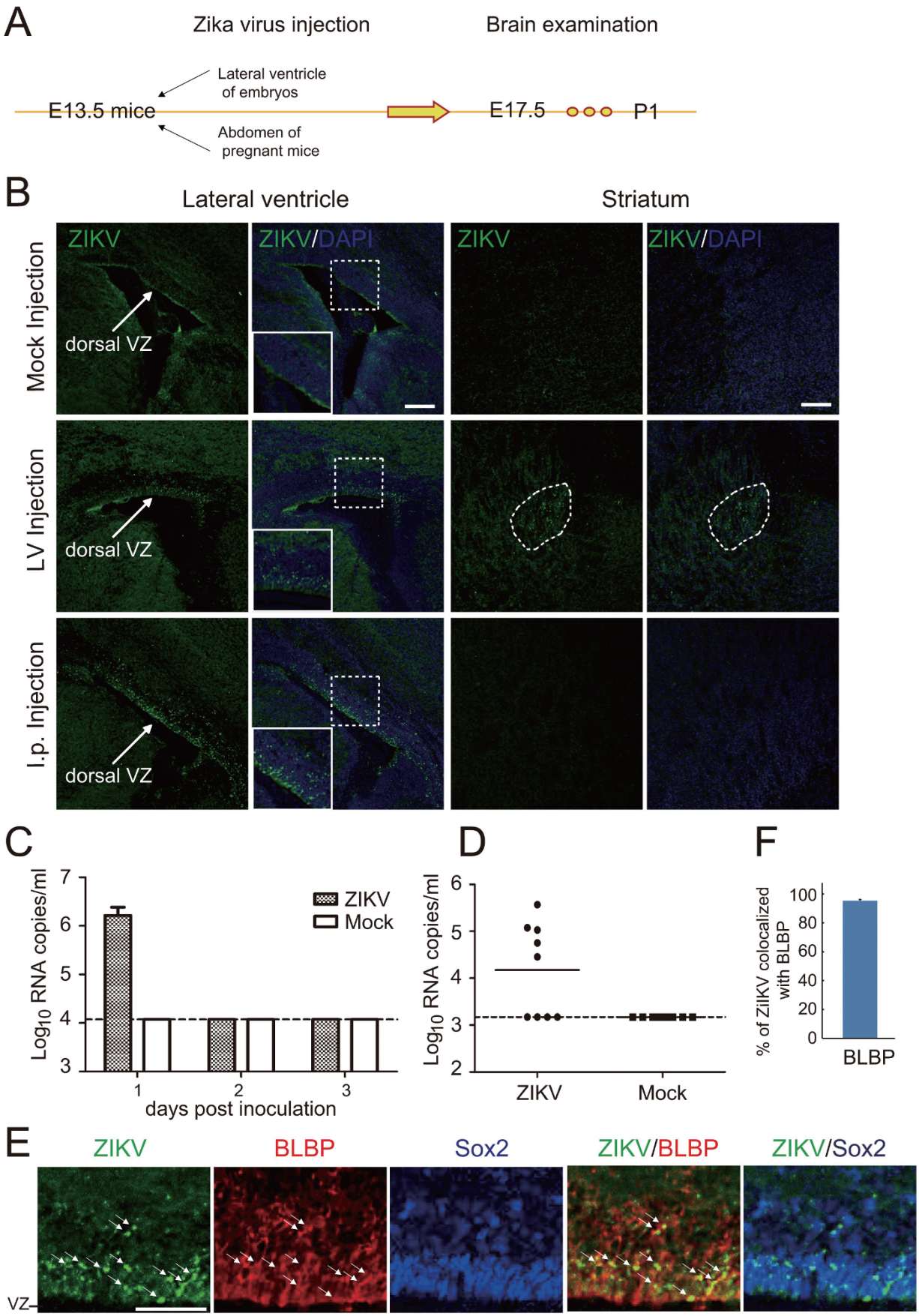
A
Zika virus injection
Brain examination
Lateral ventricle of embryos
E13.5 mice
Abdomen of pregnant mice
E17.5
P1
B
Lateral ventricle
Striatum
ZIKV
ZIKV/DAPI
Mock Injection
LV Injection
I.p. Injection
dorsal VZ
C
Log10 RNA copies/ml
ZIKV
Mock
days post inoculation
D
Log10 RNA copies/ml
ZIKV
Mock
F
% of ZIKV colocalized with BLBP
BLBP
E
ZIKV
BLBP
Sox2
ZIKV/BLBP
ZIKV/Sox2
VZ

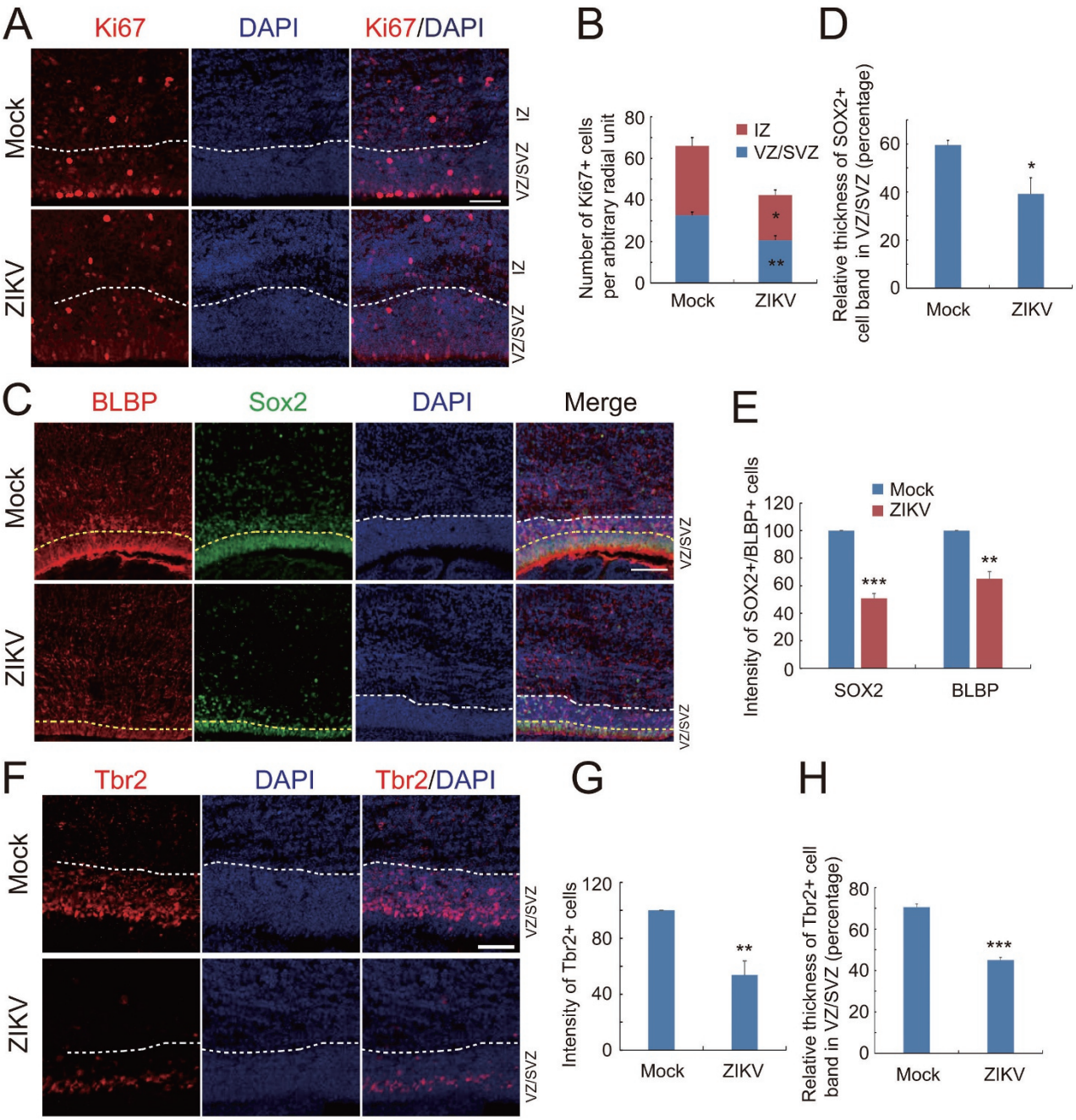

Figure 2 ZIKV inhibits neural stem cell proliferation and depletes progenitor pool in dorsal ventricular zone. **(A)** Immunostaining for Ki67 in brain slices from P1 mice i.p. injected with ZIKV or mock control at E13.5. White dash lines indicate the boundary between VZ/SVZ and IZ zones. Scale bar, 50 μm. **(B)** Quantification for the number of Ki67-positive (Ki67+) cells in VZ/SVZ and IZ regions from mock and ZIKV groups. Data are shown as mean ± SEM (**P* < 0.05, ***P* < 0.01; Student's *t*-test). **(C)** Immunostaining for BLBP and Sox2 in brain slices from P1 mice i.p. injected with ZIKV or mock control at E13.5. White dash lines indicate the boundary between VZ/SVZ and IZ zones. Yellow dash lines indicate the densely arrayed continuous Sox2-positive (Sox2+) cell layers within the VZ/SVZ region. Scale bars, 50 μm. **(D, E)** Quantification for the band thickness of densely arrayed Sox2+ cell layers relative to that of the entire VZ/SVZ region **(D)** and the intensity of Sox2+ or BLBP+ cells **(E)**. Data are mean ± SEM (**P* < 0.05, ***P* < 0.01, ****P* < 0.001, Student's *t*-test). **(F)** Immunostaining for Tbr2 in brain slices from P1 mice i.p. injected with ZIKV or mock control at E13.5. White dash lines indicate boundary between VZ/SVZ and IZ zones. Scale bars, 50 μm. **(G, H)** Quantification of relative intensity of Tbr2+ cells **(G)** and the band thickness of densely arrayed Tbr2+ cell layers relative to that of the entire VZ/SVZ region **(H)**. Data are mean ± SEM (***P* < 0.05, ****P* < 0.001, Student's *t*-test).

marked by Tbr2 constitute another type of cortical progenitor, which undergoes terminal cell division to become neurons or glia. We found that both the intensity and band thickness of Tbr2-positive IPs were also markedly reduced in the ZIKV-infected fetal brains (Figure 2F-2H). Taken together, maternal ZIKV infection caused a marked reduction of the cortical neural progenitors in the fetal mice.

Effects of ZIKV infection on expression of microcephaly or cell cycle-related genes

Genetic analysis has led to identification of a number of gene mutations associated with autosomal recessive primary microcephaly (MCPH), and most of these genes directly regulate cell cycle progression [23]. Does ZIKV infection have any effect on the expression of these MCPH-associated genes? Notably, quantitative gene expression analysis using real-time PCR showed that mRNA levels of *Microcephalin*, *CDK5RAP2*, *CASC5*, *ASPM*, *CENPJ*, *STIL*, *CEP135*, *STIL*, as well as a cell cycle-related gene *CDK6*, were downregulated to varying degrees in ZIKV-infected fetal brain samples (Figure 3A). It is known that some viral infections during pregnancy are correlated with malfunction of the brain in the offspring [24-26]. Recently, a provocative study showed that immune activation in pregnant mice can affect the cortex development of the offspring through the interleukin-17a (IL17a) pathway [27]. Interestingly, we found a marked increase in the expression of IL17Ra, the receptor of IL17a in ZIKV-infected fetal brain samples (Figure 3A). These results suggest a complex mechanism underlying the effects of ZIKV infection on mouse brain development. To further understand the impact of ZIKV infection on gene transcription network, we compared global transcriptome profiles between ZIKV-infected and mock-infected fetal mouse brains (Figure 3B and 3C; Supplementary information, Tables S1 and S2). We found that many genes involved in regulating immune responses, including innate immune reactions, and cell death program were upregulated (Figure 3B and Supplementary information, Table S1), whereas genes critical for cell proliferation and negative regulators of apoptotic process were down-regulated (Figure 3C and Supplementary information, Table S2). These changes in gene expression are similar to what was observed in cultured human neural progenitors infected by ZIKV [14], suggesting the mechanisms for ZIKV's effects on neural progenitors may be conserved among different species.

ZIKV infection causes malformation of the fetal brain

We further determined whether this maternal ZIKV infection could cause any defects in the cortical development of fetal mice. Figure 4A shows serial coronal sections of fetal brains in various anterior-posterior positions stained with DAPI. We found that outer perimeters of the cortex of ZIKV-infected fetal mice were significantly shorter than that of mock-injected control mice (Figure 4A and 4B). Interestingly, ZIKV-infected fetal mice exhibited a markedly reduced cavity of lateral ventricles accompanied by decreased ventricular surfaces compared with control mice (Figure 4A, 4C and 4D). These morphological alterations might be due to diminished ZIKV-infected RGs and the consequent reduction in proliferative neural progenitor pools along the VZ surface. Notably, we did not observe apparent changes in relative thickness of individual cortical layers (Figure 4E and 4F). We predict that the remaining ZIKV-resistant RG cells, if any, may maintain normal mode of division, radial migration and maturation, which give rise to normal lamination of fetal brains.

Discussion

ZIKV is neurotropic for the adult mouse brain, infecting neurons and astrocytes [28, 29], thus causing neurological symptoms [30, 31]. Interestingly, a historical ZIKV strain isolated prior to the 2015 epidemic can infect induced human neural progenitors with high efficiency but infect differentiated young neurons with only low efficiency [14]. Here we show that a contemporary ZIKV strain isolated from the 2015 epidemic area can be vertically transmitted from the infected pregnant mice to their fetuses, where it specifically infects the cortical neural progenitors in the brain. The vertical transmission model of ZIKV infection in mice supports well the human ZIKV cases and provides a useful platform for testing potential antiviral drugs. It is necessary to systemically analyze whether variations in different strains can affect the infection efficiency in different cell types. These analyses may provide further insights into the varying frequencies of microcephaly in different Zika virus epidemics.

Humans are different from rodents in several aspects of the cortex development, such as longer cell cycle length, longer duration of cortical neurogenesis, bigger brain surface area, and complex gyrencephalic instead of lissencephalic configuration [32]. The recently observed outer or basal radial glia cells in the massively expanded outer SVZ in primates have been considered to be associated with cortex expansion and evolution [33, 34]. Notably, mice with gene mutations associated with human microcephaly often exhibit milder phenotypes in cortex development than human patients [35, 36]. Furthermore, the reduction of the lateral ventricles in vertically infect-

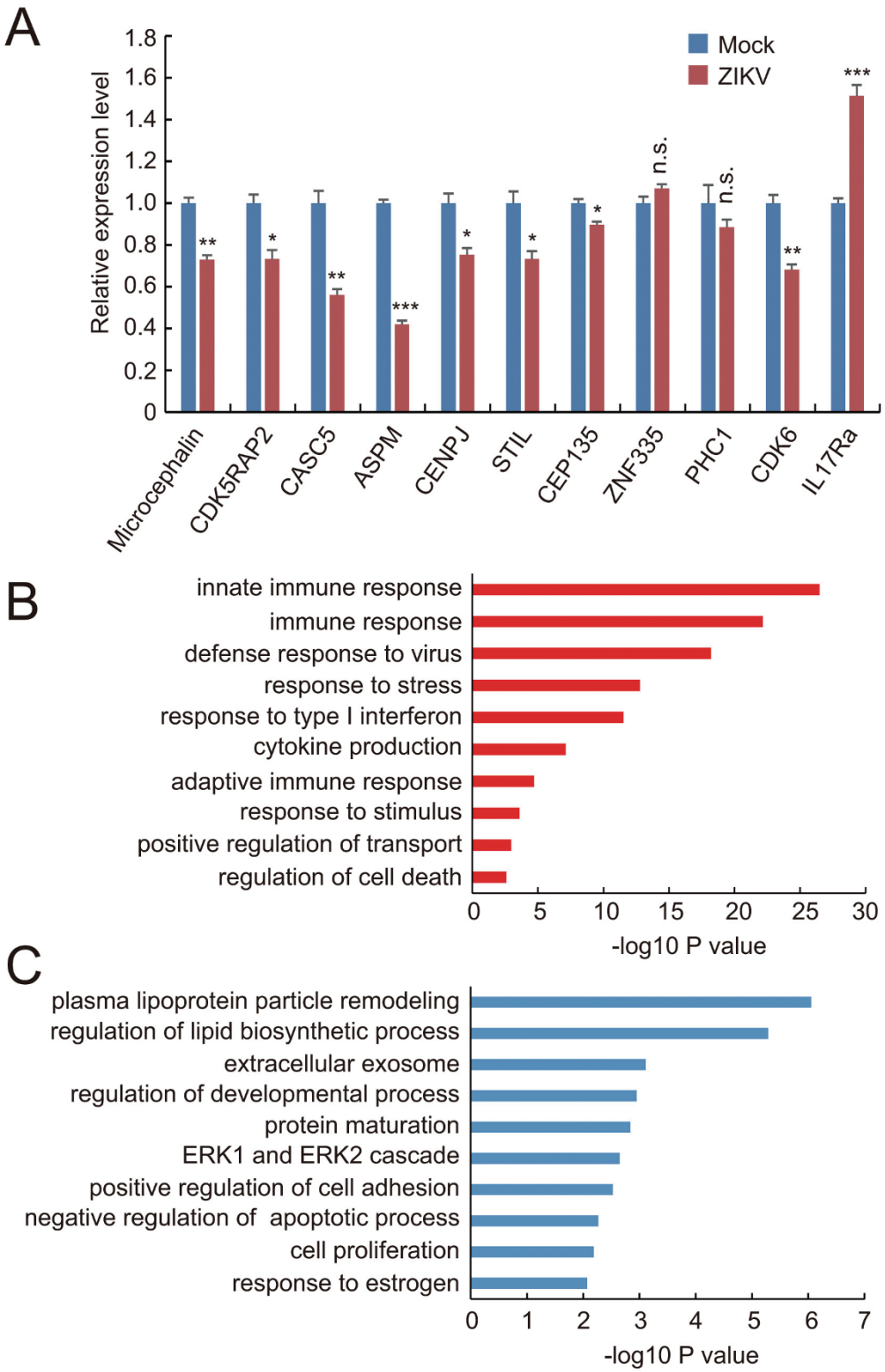

Figure 3 Effects of ZIKV infection on gene expression. **(A)** Quantitative real-time PCR analysis of the mRNA levels of cell cycle-related and microcephaly-related genes in ZIKV-injected E17.5 fetal brains. GAPDH was used as the internal control. Data are mean ± SEM from 3 experiments (*P < 0.05, **P < 0.01, ***P < 0.001, NS, no significant difference, Student's t-test). **(B, C)** RNA-seq and GO analyses reveal pathways that are significantly up-regulated **(B)** and significantly down-regulated **(C)** in ZIKV-injected E17.5 fetal brains compared with control samples. Bar plots show the –log10 P values of each term of genes.

ed offspring mice is in contradiction with the phenotype of ventriculomegaly found in newborn ZIKV patients with microcephaly [6]. This discrepancy is likely due to a species difference between humans and mice.

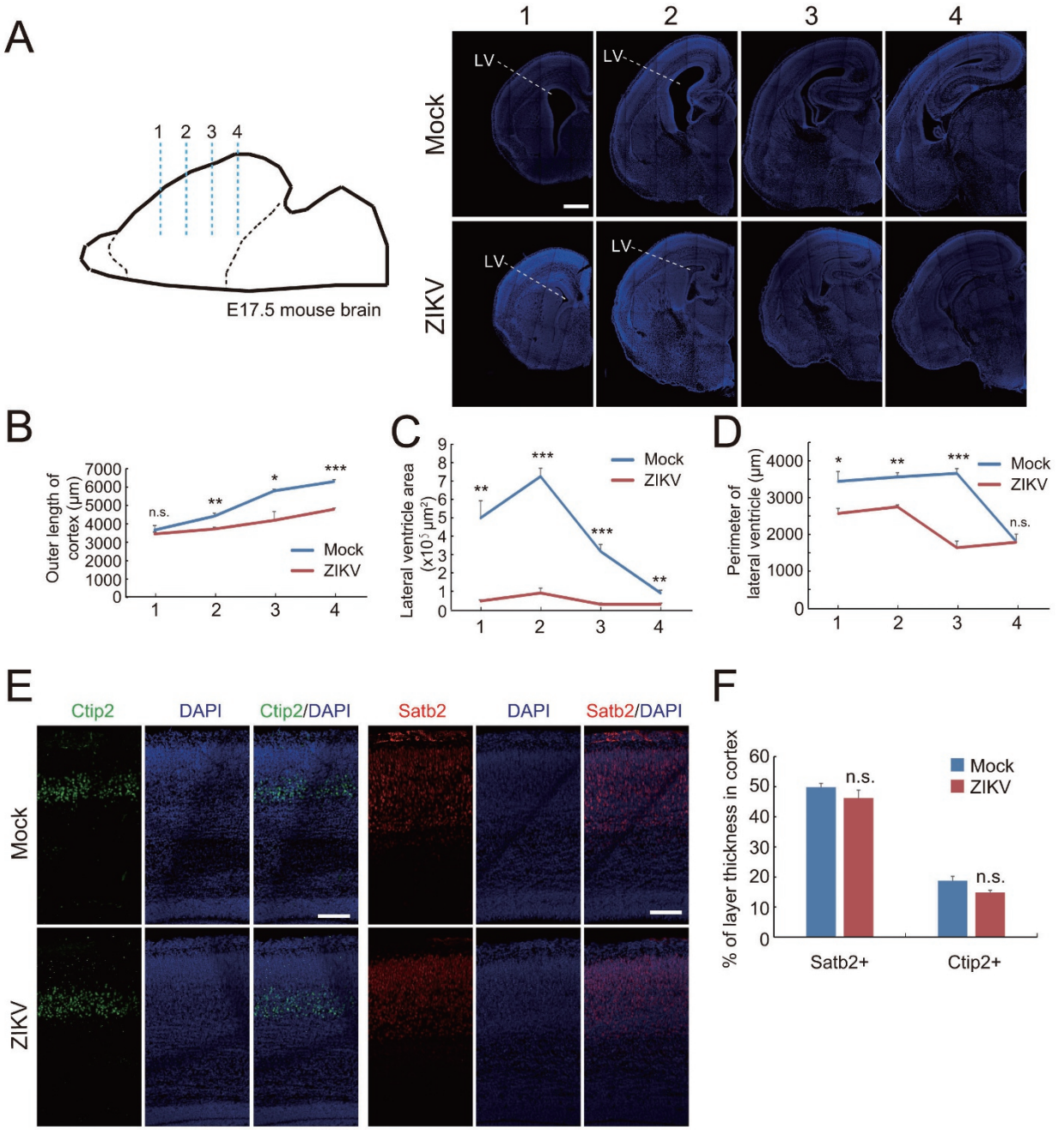

Figure 4 Effect of ZIKV infection on brain development of fetal mice. **(A)** Serial coronal brain sections as illustrated (left) were stained with DAPI (right). Numbers indicate selected corresponding sections. Scale bar, 500 μm. **(B-D)** Quantification of the length of outer cortical surface **(B)**, the lateral ventricle area **(C)**, and the perimeter lining the ventricular surface **(D)** in indicated sections. Data are shown as mean ± SEM from three offspring mice (*$P < 0.05$, **$P < 0.01$, ***$P < 0.001$, NS, no significant difference, Student's *t*-test). **(E)** E17.5 brain slices in corresponding position from mock or ZIKV-infected group were stained with antibodies against superfical layer marker Satb2 or deep layer marker Ctip2, respectively. Scale bar, 100 μm. **(F)** Quantification of the relative thickness of Satb2 or Ctip2 positive layers relative to the total cortex expressed as a percentage with the thickness of the entire cortex being 100%. There is no significant difference between two groups in each layer.

In this study, ZIKV was i.p. injected into the pregnant mice at E13.5, a stage when the most prominent cortical neurogenesis occurs. We could not rule out the possibility that injection at an earlier stage or a higher dosage might cause a stronger phenotype. The quick decline in viremia (see Figure 1C) probably mediated by the immune responses in the mother may partly account for the mild phenotype. Indeed, mice lacking components of the antiviral response have been shown to sustain higher viral loads than immunocompetent mice [30]; they may serve as a more ideal model for investigating the effect of ZIKV on fetal brain development.

In summary, we show that maternal infected ZIKV can cross the mouse placental barrier and infect RG cells in the fetal brain, causing either directly or indirectly a reduction in the proliferative pool of cortical neural progenitors, and leading to a discernable brain developmental defect in the offspring. This study thus provides a useful animal model for the screening and evaluation of therapeutic or preventive drugs and vaccines that can combat ZIKV infection.

Materials and Methods

Zika virus preparation and mouse infection

Zika virus used in this study was isolated from an imported Chinese patient returning from Samoa in February 2016 [19]. Virus stocks were prepared in mosquito C6/36 cell and stored in aliquots at −80 °C. The titer of ZIKV was determined by standard plaque forming assay on Vero cells. Real-time RT-PCR was performed to quantify viral RNA with the following primers (5′-GGTCAGCGTCCTCTCTAATAAACG-3′ and 5′-GCACCCTAGTGTCCACTTTTTCC-3′) and a fluorogenic probes (5′-FAM-AGCCATGACCGACACCACACCGT-BQ1-3′).

Approximately 10-week-old pregnant C57 mice at E13.5 were used as recipients for ZIKV infection through either i.p. injection with 300 μl virus (3×10^5 PFU/ml) or in utero injection with 1.5 μl virus into the lateral ventricles (LV) of the fetal brain. To carry out this latter procedure, C57 pregnant mice were anesthetized with pentobarbital sodium, the embryos in uterus were exposed, and 1.5 μl virus mixed with Fast Green was injected into the lateral ventricle of embryonic brain. An equal amount of vehicle DMEM was used for mock infection. Blood samples were collected for viremia analysis at 1, 2 and 3 days post infection. At 3 days post inoculation, the placentas of each embryo was dissected to determine viral RNA replication. Injected mice were raised until E17.5 or P1 for fetal brain examination. Mice injection was approved by Institutional Animal Care and Use Committee and conducted in biological safety protection laboratory.

Immunohistochemistry

The brains of E17.5 or P1 offspring mice were perfused and then post-fixed for 72 h with 4% PFA (pH7.4). The fixed mouse brains were cryoprotected in 30% sucrose solution and sectioned using a cryostat microtome at the thickness of 30 μm. The brain slices were washed with PBS and then incubated in 0.3% Triton X-100 for 30 min at room temperature. After blocking with 10% goat serum, the slices were incubated in primary antibodies at 4 °C overnight. The used primary antibodies were: mouse anti-BLBP (Abcam, 1:500), rat anti-Ctip2 (Abcam, 1:500), rabbit anti-Ki67 (Abcam, 1:500), rabbit anti-Pax6 (Covance, 1:1 000), mouse anti-Satb2 (Abcam, 1:1 000), rabbit anti-Sox2 (Millipore, 1:1 000), rabbit anti-Tbr2 (Abcam, 1:500), convalescent phase serum from the ZIKV patient (1:700). In the next day, the slices were incubated with Alexa Fluor 555/488/647 conjugated secondary antibodies (Invitrogen) for 2 h at room temperature. DAPI was obtained from Beyotime Biotechnology. Images were acquired using a Nikon A1 Plus confocal microscope with a 20× or 40× objective lens.

RNA extraction and real-time PCR

The dissociated mouse brains were ground in DMEM medium containing 2% fetal bovine serum (Life Technologies), and total RNA was extracted using PureLink RNA Mini Kit (Invitrogen) following the manufacturer's instructions. Quantitative real-time PCR (qRT-PCR) assays were used to detect the changes in expression of candidate genes following ZIKV infection. Real-time PCR was performed in 96-well plates using a Roche LightCycler 480 instrument. GAPDH was used as the reference gene for internal control. The specific primers were as follows: STIL (forward: 5′-CCTTGTGAGAGTAGGACGCC-3′, reverse: 5′-TGGGAGGATCTCTTCACTGGA-3′), CDK5RAP2 (forward: 5′-CAGCAAGATGGCAGCAAATG-3′, reverse: 5′-GTCACAGGAGAGCGAGTCAA-3′), IL17Ra (forward: 5-AATACCACAGTTCCCAAGCCAG-3′, reverse: 5′-CAGGTCTGCTACGGGCAAG-3′), PHC1 (forward: 5′-CCATCGGGGTCAAGAGGAC-3′, reverse: 5′-TGATGCCCTGTAACTCTGGC-3′), CDK6 (forward: 5′-ACGTGGTCAGGTTGTTTGATG-3′, reverse: 5′-CGGGCTCTGGAACTTTATCC-3′), ASPM (forward: 5′-CCGTACAGCTTGCTCCTTGT-3′, reverse: 5′-GGCGTTGTCCAATATCTTTCCA-3′), Microcephalin (forward: 5′-AAGAAGAAAAGCCAACGAGAACA-3′, reverse: 5′-CTCGGGTGCGAATGAAAAGC-3′), CASC5 (forward: 5-TCGCTGAAGTGGAAACAGAAAC-3′, reverse: 5′-TATCTGAGCAAGGGTCTGCG-3′), CENPJ (forward: 5′-TGGATGCCTGGAAGAGAGCA-3′, reverse: 5′-TAGATAGATTTCCTTGTGCTGGC-3′), CEP135 (forward: 5′-CCAAAGCCGAGAAACCTCCA-3, reverse: 5′-ATTGCTCGCTCTCGTTCGTA-3′), ZNF335 (forward: 5′-GCCAACCGCAGATTCAAGTG-3′, reverse: 5′-GAAGGTGCGGTAGGGACAAA-3′), GAPDH (forward: 5′-GTGAAGCAGGCATCTGAGGG-3′, reverse: 5′-GCCGTATTCATTGTCATACCAGG-3′).

RNA-seq and transcriptome analysis

Whole ZIKV-infected E17.5 fetal brains or mock control at E13.5 were subject to RNA-seq and transcriptome analysis. Briefly, total RNA was extracted using PureLink RNA Mini Kit (Invitrogen) according to the manufacturer's instructions, quantified using NanoDrop ND-2000, and checked for RNA integrity by an Agilent Bioanalyzer 2100 (Agilent Technologies, Santa Clara, CA, USA). RNA libraries were generated using TruSeq Stranded RNA Sample Prep Kit (Illumina) following manufacturer's protocol, quantified with Qubit 2.0 Fluorometer (Invitrogen), examined for dot distribution with Agilent 2100, and subjected to sequencing using Illumina Hiseq 2000. Acquired data were processed to obtain raw reads, which were then extracted for genome mapping with

TopHat (version 2.0.9) [37]. Genes with differential expression levels were identified using edgeR [38], with GO enrichment and KEGG pathway enrichment analyses.

Acknowledgments

We thank Dr Fu-Chun Zhang at Guangzhou No.8 People's hospital for providing the convalescent serum from the recovered patient. This study was partially supported by grants from, the National Natural Science Foundation of China (31330032, 31490591, 31321091, and 61327902 to ZGL, 31371063 to KYW, 81522025 and 8151101191 to CFQ), the National Key Basic Research Program of China (2014CB910203), the Strategic Priority Research Program of the Chinese Academy of Sciences (XDB02040003), the Youth Innovation Promotion Association CAS (2016247 to KYW), and the Newton Advanced Fellowship from the UK Academy of Medical Sciences (to CFQ).

Author Contributions

KYW, QY, and XYH performed virus injection. KYW and GLZ did brain sectioning, immunostaining, real-time PCR and RNA-seq analyses. YQD and XFL amplified and titered virus and helped with virus injection. ZGL, WCC, and CFQ conceived of the research. ZGL, CFQ and KYW wrote the manuscript with inputs and comments from all authors.

Competing Financial Interests

The authors declare no competing financial interests.

References

1 Oehler E, Fournier E, Leparc-Goffart I, *et al*. Increase in cases of Guillain-Barre syndrome during a Chikungunya outbreak, French Polynesia, 2014 to 2015. *Euro Surveill* 2015; **20**:30079.
2 Ioos S, Mallet HP, Leparc Goffart I, *et al*. Current Zika virus epidemiology and recent epidemics. *Med Mal Infect* 2014; **44**:302-307.
3 Wang L, Valderramos SG, Wu A, *et al*. From mosquitos to humans: genetic evolution of Zika virus. *Cell Host Microbe* 2016 Apr 14. doi:10.1016/j.chom.2016.04.006.
4 Oliveira Melo AS, Malinger G, Ximenes R, Szejnfeld PO, Alves Sampaio S, Bispo de Filippis AM. Zika virus intrauterine infection causes fetal brain abnormality and microcephaly: tip of the iceberg? *Ultrasound Obstet Gynecol* 2016; **47**:6-7.
5 Fauci AS, Morens DM. Zika Virus in the Americas--yet another arbovirus threat. *N Engl J Med* 2016; **374**:601-604.
6 Hazin AN, Poretti A, Cruz DD, *et al*. Computed tomographic findings in microcephaly associated with Zika virus. *N Engl J Med* 2016 Apr 6. doi:10.1056/NEJMc1603617
7 Schuler-Faccini L, Ribeiro EM, Feitosa IM, *et al*. Possible association between Zika virus infection and microcephaly - Brazil, 2015. *MMWR* 2016; **65**:59-62.
8 Mlakar J, Korva M, Tul N, *et al*. Zika virus associated with microcephaly. *N Engl J Med* 2016; **374**:951-958.
9 Driggers RW, Ho CY, Korhonen EM, *et al*. Zika virus infection with prolonged maternal viremia and fetal brain abnormalities. *N Engl J Med* 2016. doi: 10.1056/NEJMoa1601824
10 Mecharles S, Herrmann C, Poullain P, *et al*. Acute myelitis due to Zika virus infection. *Lancet* 2016; **387**:1481.
11 Heymann DL, Hodgson A, Sall AA, *et al*. Zika virus and microcephaly: why is this situation a PHEIC? *Lancet* 2016; **387**:719-721.
12 Faria NR, Azevedo RD, Kraemer MU, *et al*. Zika virus in the Americas: early epidemiological and genetic findings. *Science* 2016; **352**:345-349.
13 Cauchemez S, Besnard M, Bompard P, *et al*. Association between Zika virus and microcephaly in French Polynesia, 2013-15: a retrospective study. *Lancet* 2016 Mar 15. doi:10.1016/S0140-6736(16)00651-6.
14 Tang H, Hammack C, Ogden SC, *et al*. Zika virus infects human cortical neural progenitors and attenuates their growth. *Cell Stem Cell* 2016 May 5. doi:10.1016/j.stem.2016.02.016.
15 Garcez PP, Loiola EC, Madeiro da Costa R, *et al*. Zika virus impairs growth in human neurospheres and brain organoids. *Science* 2016 Apr 10. doi: 10.1126/science.aaf6116
16 Qian X, Nguyen Ha N, Song MM, *et al*. Brain-Region-Specific organoids using mini-bioreactors for modeling ZIKV exposure. *Cell* 2016 Apr 21. doi:10.1016/j.cell.2016.04.032.
17 Nowakowski TJ, Pollen AA, Di Lullo E, *et al*. Expression analysis highlights AXL as a candidate Zika virus entry receptor in neural stem cells. *Cell Stem Cell* 2016 May 5. doi:10.1016/j.stem.2016.03.012.
18 Faye O, Diallo D, Diallo M, Weidmann M, Sall AA. Quantitative real-time PCR detection of Zika virus and evaluation with field-caught mosquitoes. *Virol J* 2013; **10**:311.
19 Deng YQ, Zhao H, Li XF, *et al*. Isolation, identification and genomic characterization of the Asian lineage Zika virus imported to China. *Sci China Life Sci* 2016; **59**:428-430.
20 Musso D. Zika virus transmission from French Polynesia to Brazil. *Emerg Infect Dis* 2015; **21**:1887.
21 Calvet G, Aguiar RS, Melo AS, *et al*. Detection and sequencing of Zika virus from amniotic fluid of fetuses with microcephaly in Brazil: a case study. *Lancet Infect Dis* 2016 Feb 17. doi:10.1016/S1473-3099(16)00095-5.
22 Martines RB, Bhatnagar J, Keating MK, *et al*. Notes from the field: evidence of Zika virus infection in brain and placental tissues from two congenitally infected newborns and two fetal losses - Brazil, 2015. *MMWR* 2016; **65**:159-160.
23 Thornton GK, Woods CG. Primary microcephaly: do all roads lead to Rome? *Trends Genet* 2009; **25**:501-510.
24 Atladottir HO, Thorsen P, Ostergaard L, *et al*. Maternal infection requiring hospitalization during pregnancy and autism spectrum disorders. *J Autism Dev Disord* 2010; **40**:1423-1430.
25 Brown AS, Sourander A, Hinkka-Yli-Salomaki S, *et al*. Elevated maternal C-reactive protein and autism in a national birth cohort. *Mol Psychiatry* 2014; **19**:259-264.
26 Malkova NV, Yu CZ, Hsiao EY, Moore MJ, Patterson PH. Maternal immune activation yields offspring displaying mouse versions of the three core symptoms of autism. *Brain Behav Immun* 2012; **26**:607-616.
27 Choi GB, Yim YS, Wong H, *et al*. The maternal interleukin-17a pathway in mice promotes autism-like phenotypes in offspring. *Science* 2016; **351**:933-939.
28 Dick GW, Kitchen SF, Haddow AJ. Zika virus. I. Isolations and serological specificity. *Trans R Soc Trop Med Hyg* 1952; **46**:509-520.

29 Bell TM, Field EJ, Narang HK. Zika virus infection of the central nervous system of mice. *Arch Gesamte Virusforsch* 1971; **35**:183-193.
30 Lazear Helen M, Govero J, Smith AM, *et al*. A mouse model of Zika virus pathogenesis. *Cell Host Microbe* 2016 Apr 5. doi:10.1016/j.chom.2016.03.010.
31 Rossi SL, Tesh RB, Azar SR, *et al*. Characterization of a Novel Murine Model to Study Zika Virus. *Am J Trop Med Hyg* 2016 Mar 28. doi: 10.4269/ajtmh.16-0111
32 Geschwind DH, Rakic P. Cortical evolution: judge the brain by its cover. *Neuron* 2013; **80**:633-647.
33 Hansen DV, Lui JH, Parker PR, Kriegstein AR. Neurogenic radial glia in the outer subventricular zone of human neocortex. *Nature* 2010; **464**:554-561.
34 Fietz SA, Kelava I, Vogt J, *et al*. OSVZ progenitors of human and ferret neocortex are epithelial-like and expand by integrin signaling. *Nat Neurosci* 2010; **13**:690-699.
35 Lizarraga SB, Margossian SP, Harris MH, *et al*. Cdk5rap2 regulates centrosome function and chromosome segregation in neuronal progenitors. *Development* 2010; **137**:1907-1917.
36 Pulvers JN, Bryk J, Fish JL, *et al*. Mutations in mouse Aspm (abnormal spindle-like microcephaly associated) cause not only microcephaly but also major defects in the germline. *Proc Natl Acad Sci USA* 2010; **107**:16595-16600.
37 Trapnell C, Pachter L, Salzberg SL. TopHat: discovering splice junctions with RNA-Seq. *Bioinformatics* 2009; **25**:1105-1111.
38 Robinson MD, McCarthy DJ, Smyth GK. edgeR: a Bioconductor package for differential expression analysis of digital gene expression data. *Bioinformatics* 2010; **26**:139-140.

(**Supplementary information** is linked to the online version of the paper on the *Cell Research* website.)